

# FeatureSORT: Essential Features for Effective Tracking

Hamidreza Hashempoor, Rosemary Koikara, Yu Dong Hwang

**Abstract**—In this work, we introduce a novel tracker designed for online multiple object tracking with a focus on being simple, while still being effective. We provide multiple feature modules each of which stands for a particular appearance information. By integrating distinct appearance features, including clothing color, style, and target direction, alongside a ReID network for robust embedding extraction, our tracker significantly enhances online tracking accuracy. Additionally, we propose the incorporation of a stronger detector and also provide advanced post processing methods that further elevate the tracker’s performance. During real-time operation, we establish measurement-to-track associated distance function which includes the IoU, direction, color, style, and edge (ReID features) similarity information, where each metric is calculated separately. With the design of our feature-related distance function, it is possible to track objects through longer periods of occlusions, while keeping the number of identity switches comparatively low. Extensive experimental evaluation demonstrates notable improvements in tracking accuracy and reliability, as evidenced by reduced identity switches and enhanced occlusion handling. These advancements not only contribute to the state-of-the-art in object tracking but also open new avenues for future research and practical applications demanding high precision and reliability.

**Index Terms**—Visual Tracking, DeepSORT

## I. INTRODUCTION

The purpose of MULTI-OBJECT TRACKING (MOT) is to detect and track all objects in each frame. This task plays an essential role in video understanding. Due to the sophisticated nature of videos that include several objects, detected bounding boxes are not accurate since detectors are vulnerable to making imperfect predictions. Moreover, MOT methods [1]–[5] need to deal with true positive, false positive balance in detection boxes to remove low confidence detection boxes and only process high confidence score objects [6], [7]. Thanks to the proliferation of strong detection modules in recent years, handling this issue has become feasible. Tracking-by-detection (TBD) is now the most effective paradigm for MOT. Since MOT relies heavily on both object detection and object re-identification (ReID), most TBD methods invest significantly in state-of-the-art (SOTA) detectors and ReID models to enhance MOT performance [8]. These methods first extract appearance and motion information of the objects, then use a matching algorithm to assign detections to the existing tracklets.

Following along the same lines, this paper presents a simple but effective MOT baseline called FeatureSORT. We elevate the classic TBD tracker, DeepSORT [3], which is among

the foundational approaches that integrate a deep learning model into the MOT task. DeepSORT is a simple, explainable, and effective model that has widespread applications across computer vision tasks tracking objects. While there are critics of DeepSORT for its old-fashioned tracking algorithm, DeepSORT has a great capacity to be reinforced with newer features and inference approaches. To be specific, firstly we provide a stronger detector with better embedding [9] for DeepSORT. Second, in addition to the ReID features, we equip DeepSORT with separated feature modules each of which stands for a particular feature of the pedestrian targets. Despite the effectiveness of ReID networks for extracting embedding information of each target, this information is too generic and may not be enough to include the whole appearance information of the target, e.g. colors, direction, style, etc. Third, we also include advanced post processing methods from recent works to further improve DeepSORT’s performance. Enhancing DeepSORT with these simple but effective components establish the proposed FeatureSORT, and it is shown that FeatureSORT can achieve SOTA results on the popular benchmarks MOT16 [10], MOT17 [11] and MOT20 [12] based on the features that we use.

The motivations for FeatureSORT can be summarized as follows:

- 1) To address the limitations of existing TBD trackers by creating a modular, feature-based tracking framework. Our goal is to establish a versatile baseline that can be readily adapted and improved using various tracking methodologies.
- 2) To enhance the adaptability and effectiveness of MOT systems in varying environments. FeatureSORT aims to establish a new benchmark for performance comparison in the MOT field.
- 3) To showcase how the strategic selection and application of advanced inference and post processing methods can substantially enhance tracking accuracy and efficiency.

In the context of MOT, two predominant challenges are *missing association* and *missing detection*, as identified by Du et al. [13]. *Missing association* is the existence of the same object in more than one track trajectory. This problem is prevalent in online trackers due to their lack of access to comprehensive global information for association. The second challenge, *missing detections*, also known as false negatives, refers to when the object is mistakenly classified as background. This misclassification can be attributed to factors such as occlusions and low resolutions.

After the online tracking algorithm, each trajectory of an object can be split into several short and long-missing

H. Hashempoor, R. Koikara and Y. Hwang are with Pintel Co. Ltd., Seoul, South Korea (e-mail: {Hamidreza, Rosemary, Ydhwang}@pintel.co.kr).  
Manuscript revised July, 2024.

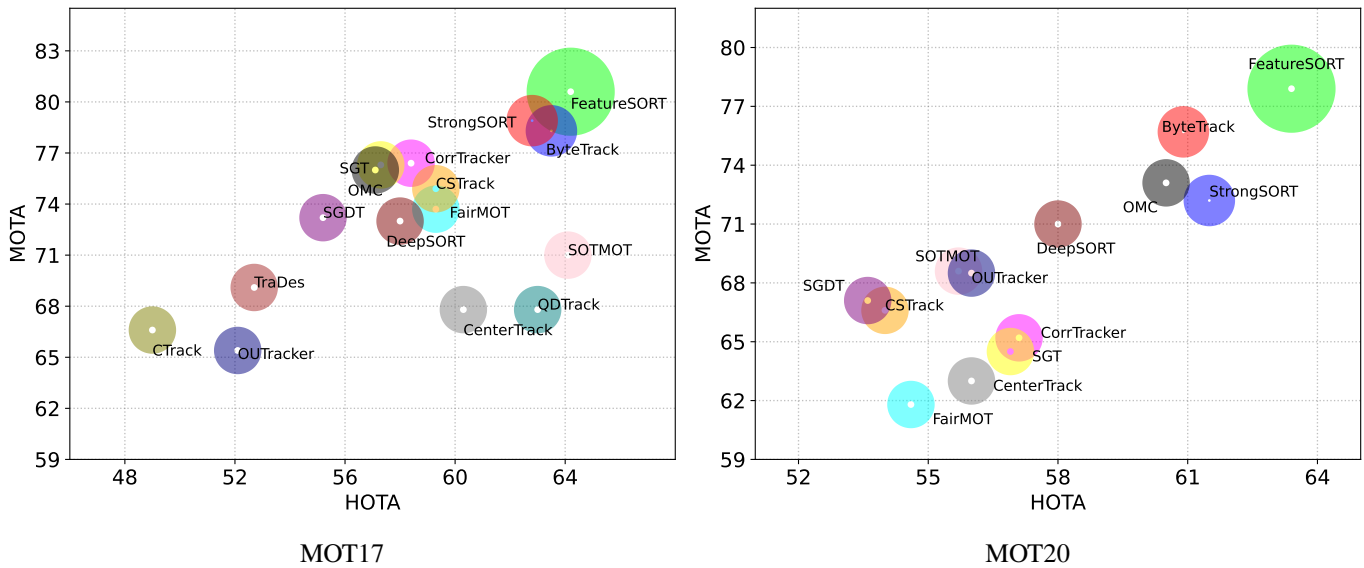


Fig. 1: MOTA-HOTA comparisons of SOTA trackers with FeatureSORT (ours) on MOT17 and MOT20 test sets without offline post-processing.

associated tracklets due to detection errors or object occlusion. To merge these trajectories into a single trajectory, we use global information in an offline manner. Our global link is same as GIAOTracker [14], where we propose a complex global link algorithm that encodes tracklet appearance features using an improved ResNet50-TP model [15] and associates tracklets together with spatial and temporal costs. Although this approach is computationally-intensive, linking the tracklet based on the global information is usually conducted offline, after obtaining all of tracklets.

To cope with missing-detection issue, using linear interpolation is widespread in the community, where after obtaining a trajectory, missing frames are interpolated linearly [16]–[19]. However, it ignores motion information during interpolation, which limits the accuracy of the interpolated positions. To alleviate this issue, we integrate the idea of the Gaussian Smoothing Process (GSP) [20] for the interpolation. GSP can benefit our model by modifying each observation based on both the past and future observations.

Linking and interpolation are lightweight, plug-and-play, and model-independent post-processing approaches, making them beneficial and suitable for all tracker algorithms. In our experiments, we demonstrate that applying these post-processing methods to FeatureSORT enhances tracking performance.

Although most SOTA tracker algorithms rely on offline post-processing to achieve convincing performance, we focus more on online tracking. Therefore, we present most of our results in the online scenario, assuming that post processing may not be feasible. Extensive experiments demonstrate that the proposed feature modules can create notable improvements on FeatureSORT. By applying our strengthened detector coupled with feature modules, we achieve online SOTA results on various benchmarks, i.e., MOT16, MOT17, MOT20. Figure 1 presents the MOTA-HOTA comparisons of SOTA online trackers (without offline post-processing) with our proposed

model on the MOT17 and MOT20 test sets.

The contributions of our work are mentioned as follows:

- We propose FeatureSORT, which reinforces DeepSORT with advanced detection module and feature modules (i.e., color, style, direction) alongside some inference strategy. This approach not only achieves SOTA performance on MOT benchmarks but can also serve as a robust and fair baseline for other MOT methodologies, offering significant value to the field.
- To resolve the issue of missing association and detections, we propose Global linking and GSP algorithms that can be applied offline to correct tracklet trajectory. Global linking and GSP can be plugged into various trackers to improve their performance.
- Through extensive experimentation, we validate the effectiveness of our proposed methods in enhancing visual tracking capabilities. Furthermore, the integration of our designed feature modules, tailored to various environmental contexts, enables the proposed FeatureSORT to achieve SOTA performance across multiple benchmarks, including MOT16, MOT17, and MOT20.

The remainder of this paper is organized as follows: Section II provides an overview of the related literature. In Section III, we briefly review the DeepSORT algorithm and provide the basic background used in this paper. Section IV delves into FeatureSORT, where we explain the individual modules. Experiment setup details, along with conducted experiments and numerical results, are presented in Section V. Finally, we discuss the potential limitations of this work in Section VI and conclude the paper in Section VII.

## II. RELATED WORK

In the domain of MOT, TBD models have emerged as a cornerstone methodology. These models operate by first detecting objects in individual frames and then associating

these detections over time to form object trajectories. The efficacy of TBD models hinges significantly on the association mechanism, which attempts to match detections across frames based on various types of information. This process is fraught with challenges, including occlusions, fast-moving objects, and changes in appearance or illumination.

We categorize TBD models into three classes according to the type of information utilized for association. This classification not only aids in understanding the landscape of existing approaches but also highlights the evolution of methodologies.

#### A. Location and Motion information based Methods

SORT [21] utilizes the Kalman Filter [22], a form of Gaussian filtering, to estimate the next locations of tracklets. It then assesses the overlap of tracklets with current detections and utilizes a matching algorithm to assign current detections to tracklets. The IoU-Tracker [23] computes the overlap between the tracked object's location in the last frame and the detections, without relying on Gaussian filtering to estimate the next locations. Both SORT and IoU-Tracker are widely used in practical applications because of their simplicity and ease of implementation. However, they may not be the optimal choices for challenging scenarios, such as crowded scenes or fast motion. A group of works, such as [4], [24]–[26] consider intricate single-object tracking methods to obtain precise object locations. These approaches are significantly slow, especially when numerous objects in the scene need to be tracked. To tackle the challenges posed by missing trajectories and fragments of tracklets, Zhang et al. [27] propose a motion evaluation network that learns the features of tracklets over extended periods, facilitating effective association. MAT [28], an improved version of SORT, incorporates camera motion modeling and employs dynamic windows for long-range association.

#### B. Appearance information based Methods

Recent approaches [3], [29]–[32] consider cropping the image based on the detection bounding boxes and feeding the cropped images into Re-ID networks [33]–[35] to extract image embeddings. They then define a similarity metric to determine the similarity between tracklets and detection embeddings obtained from the Re-ID network, using a matching algorithm to complete the assignment. This method is adept at handling scenarios involving fast motion and occlusion. Specifically, owing to the stability of object features over relatively long periods, these models can re-initialize lost tracks.

Additionally, several studies [36]–[39] focus on improving appearance embeddings. For example, Bae et al. [36] introduce an online appearance learning method to address appearance changes over time. Tang et al. [37] incorporate body pose features to improve appearance embedding. Some algorithms, such as that by Sadeghian et al. [38], suggest combining multiple types of information (i.e. motion, appearance and location) to derive a more accurate similarity metric. MOTDT [39] introduces a hierarchical data association policy that utilizes IoU for assigning objects to tracklets when appearance features deemed unreliable. Additionally, a group of works,

including those by Mahmoudi et al. [31] and Fang et al. [40], propose more sophisticated assignment strategies, such as using recurrent neural networks for association purposes.

#### C. Offline Methods

Offline methods, also known as batch methods, [41]–[47] often achieve better results by conducting global optimization across entire trajectories, after tracking complete sequences. For example, Zhang et al. [41] construct a graphical model with nodes representing detections across various frames. They then perform a search by using the min-cost flow algorithm, which exploits the graph's specific characteristics to reach the optimum solution, surpassing the efficiency of Linear Programming. Berclaz et al. [43] treat data assigning as a flow optimization task, employing the K-shortest paths approach to tackle the issue, which eminently speeds up the computation.

Milan et al. [1] approach the problem of multi-object tracking by formulating it as the minimization of a continuous energy function, seeking an appropriate energy function. This energy function considers the locations and motion of all objects in all frames, along with associated constraints. MPNTrack [46] comprises trainable graph neural networks to conduct a global assigning of the entire set of detections. Hornakova et al. [47] define the MOT problem as a lifted disjoint path problem and suggest edges for long-range temporal interactions. This technique substantially reduces ID switches and re-identifies lost trajectories.

### III. REVIEW OF DEEPSORT ALGORITHM

In this section, we provide an overview of the DeepSORT approach, which leverages two distinct branches to extract information: one dedicated to appearance and the other to motion. For each frame, the appearance branch utilizes an appearance descriptor, pre-trained on the MARS person re-identification dataset [48], to extract the appearance embedding. This approach takes advantage of a feature bank mechanism to store the embeddings of the last frames for each tracklet. Upon detecting a new object, the smallest cosine distance between the feature bank  $\mathcal{E}^{(i)}$  of the  $i$ -th tracklet and the feature vector  $\mathbf{f}^j$  of the  $j$ -th detection is computed as:

$$\text{dist}(i, j) = \min\{1 - \langle \mathbf{e}^{(i)}, \mathbf{f}^j \rangle | \mathbf{e}^{(i)} \in \mathcal{E}^{(i)}\} \quad (1)$$

The cosine distance is later utilized in the matching cost function for assignment purposes. The motion branch uses the Gaussian filtering approach to estimate the positions of tracklets in the current frame. Gaussian filtering (Kalman filter) works in two stages: state prediction and state update. During the state prediction stage, it estimates the current state as:

$$\mu(t|t-1) = \mathbf{G}(t)\mu(t-1|t-1) \quad (2)$$

$$\mathbf{P}(t|t-1) = \mathbf{G}(t)\mathbf{P}(t-1|t-1)\mathbf{G}^T(t) + \mathbf{Q}(t) \quad (3)$$

where,  $\mathbf{G}(t)$  is the linear state transition matrix,  $\mathbf{Q}(t)$  is the covariance of the process noise,  $\mu(t-1|t-1)$  and  $\mathbf{P}(t-1|t-1)$  are the mean and covariance of the filtered state at time step

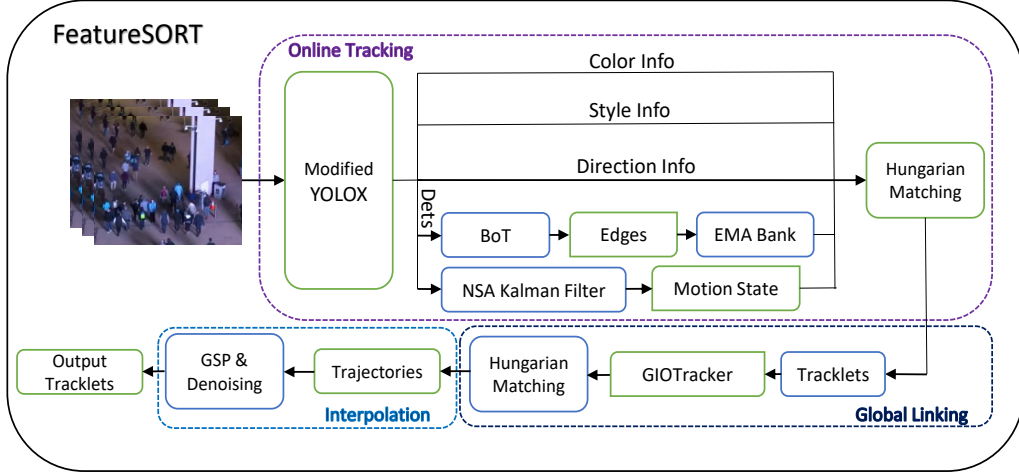


Fig. 2: Schematic diagram of FeatureSORT.

$t - 1$ , respectively, while  $\mu(t|t - 1)$  and  $\mathbf{P}(t|t - 1)$  are the predicted mean and covariance states at time step  $t$ . In the state update stage, the Kalman gain is obtained as a function of the predicted covariance of the state  $\mathbf{P}(t|t - 1)$  and the observation noise  $\mathbf{R}(t)$ :

$$\mathbf{K}(t) = \mathbf{P}(t|t - 1)\mathbf{H}^T(t)(\mathbf{H}(t)\mathbf{P}(t|t - 1)\mathbf{H}^T(t) + \mathbf{R}(t))^{-1}, \quad (4)$$

where  $\mathbf{H}(t)$  is the emission matrix. Then, the filtered state at time step  $t$  is given as follows:

$$\mu(t|t) = \mu(t|t - 1) + \mathbf{K}(t)(\mathbf{z}(t) - \mathbf{H}(t)\mu(t|t - 1)) \quad (5)$$

$$\mathbf{P}(t|t) = (\mathbf{I} - \mathbf{K}(t)\mathbf{H}(t))\mathbf{P}(t|t - 1) \quad (6)$$

where  $\mathbf{z}(t)$  is the measurement at time step  $t$ . Having obtained the motion state of tracks and new detection bounding boxes, DeepSORT uses Euclidean distance to measure the dissimilarity between them. The algorithm considers this motion distance as a criterion to filter out unlikely assignments. Subsequently, it performs the matching cascade algorithm to address the assignment task as a series of subproblems, rather than a global assignment problem. This strategy prioritizes more frequently seen objects during the matching step. Each association subproblem is solved using Hungarian algorithm.

#### IV. FEATURESORT

In this section, we present various approaches to upgrade DeepSORT [3] to FeatureSORT. Specifically, we do not claim any novel approach in this section. Rather, our contribution lies in strengthening DeepSORT with various methods to establish a more robust MOT baseline. Our enhancements over DeepSORT encompass a stronger detection model, the integration of meaningful feature modules to enhance tracking performance, the introduction of new inference strategies, and their implementation. These enhancements collectively provide the necessary tools for effective object tracking. The overall structure is depicted in figure 2. A summary table with all notations used throughout this section and their respective descriptions are provided in table I.

##### A. Stronger detector

By deploying the high-performance detector YOLOX [49], we obtain much more accurate detection results, which is a mandatory factor to achieve reliable tracking performance. Following [2], [11], [50]–[53], we train the detector on the combination of MOT15, MOT16, MOT17, MOT20, COCO, CrowdHuman [54] and ETHZ [55] datasets.

##### B. Feature-based modules

Providing feature-based modules for our tracking algorithm equips the whole system with stronger embedding information and provides more clues for both ReID and tracking consistency, useful for many scenarios like occlusion, imperfect detections, etc. The YOLOX structure is designed to propose separated heads for each of localization and classification, which constructs the whole detection procedure. We artificially add two separate heads alongside the localization and classification heads. One head is for extracting embeddings for color and style classification, while another head gives us embedding of direction classification. To maintain the high performance of the detector, we freeze the backbone, localization head, and classification head after the detection training phase, and train feature module heads separately. The modified structure of the decoupled head of YOLOX is shown in figure 3.

**Clothes Color.** First, we conduct a color annotation process for the images into 10 broad categories: 1: Black; 2: Blue; 3: Green; 4: Magenta; 5: Pink; 6: Purple; 7: Red; 8: Yellow; 9: White; 10: Navy (Deep Blue). Next, we encode the colors as a vector representing each object's clothes color. For example,  $\mathbf{gtc} = [[1 \ 0 \ 0 \ 1 \ 0 \ 0 \ 0 \ 0 \ 0 \ 0]]$  means the output color is green and black (can be interpreted as the colors of upper body and lower body clothes). Training can be completed by considering a cross-entropy loss function over the color labels:

$$\mathcal{L}_{color}(\mathbf{gtc}, \mathbf{c}) = - \sum_{k=1}^{10} \mathbf{gtc}_k \log(c_k) + (1 - \mathbf{gtc}_k) \log(1 - c_k) \quad (7)$$

where  $[\mathbf{gtc}_1, \dots, \mathbf{gtc}_{10}] = \mathbf{gtc}$  is the label corresponding to the input of network and  $[c_1, \dots, c_{10}] = \mathbf{c}$  is the output of network from the color head. After making the color annotations of

TABLE I: List of notations with meaning.

Notation	Meaning
$T^{(i)}$	Length of $i$ -th tracklet
$\mathbb{T}^{(i)}$	Length set of $i$ -th tracklet. $\mathbb{T}^{(i)} = [1, \dots, T^{(i)}]$
$SL^{(i)}$	Stack length of $i$ -th tracklet
$\mathbb{SL}^{(i)}$	Stack length set of $i$ -th tracklet. $\mathbb{SL}^{(i)} = [T^{(i)} - SL^{(i)}, \dots, T^{(i)}]$
$\mathbf{f}^j$	ReID embedding of the $j$ -th detection. $\mathbf{f}^j \in \mathbb{R}^d$
$\mathbf{F}$	ReID embedding matrix with $\mathbf{f}^j$ rows. $\mathbf{F} \in \mathbb{R}^{\text{num of obj} \times d}$
$\mathbf{f}^{(i)}$	ReID embedding of assigned object to $i$ -th tracklet. $\mathbf{f}^{(i)} \in \mathbb{R}^d$
$\mathcal{E}^{(i)}$	Target ReID embedding stack of $i$ -th tracklet. $\mathcal{E}^{(i)} \in \mathbb{R}^{SL^{(i)} \times d}$
$\mathbf{c}^j$	Predicted color label of the $j$ -th detection. $\mathbf{c}^j \in \mathbb{R}^{10}$
$\mathbf{C}$	Predicted color label matrix with $\mathbf{c}^j$ rows. $\mathbf{C} \in \mathbb{R}^{\text{num of obj} \times 10}$
$\mathbf{GTC}$	Ground truth color label matrix. $\mathbf{GTC} \in \mathbb{R}^{\text{num of obj} \times 10}$
$\mathbf{c}^{(i)}$	Predicted color label of assigned object to $i$ -th tracklet
$\mathcal{C}^{(i)}$	Clothes color stack of $i$ -th tracklet with $\mathbf{c}^{(i)}$ elements. $\mathcal{C}^{(i)} \in \mathbb{R}^{SL^{(i)} \times 10}$
$\mathbf{s}^j$	Predicted style label of the $j$ -th detection. $\mathbf{s}^j \in \mathbb{R}^{20}$
$\mathbf{S}$	Predicted color label matrix with $\mathbf{s}^j$ rows. $\mathbf{S} \in \mathbb{R}^{\text{num of obj} \times 20}$
$\mathbf{GTS}$	Ground truth style label matrix. $\mathbf{GTS} \in \mathbb{R}^{\text{num of obj} \times 20}$
$\mathbf{s}^{(i)}$	Predicted style label of assigned object to $i$ -th tracklet. $\mathbf{s}^j \in \mathbb{R}^{20}$
$\mathcal{S}^{(i)}$	Clothes style stack of $i$ -th tracklet with $\mathbf{s}^{(i)}$ elements. $\mathcal{S}^{(i)} \in \mathbb{R}^{SL^{(i)} \times 20}$
$\mathbf{p}^j$	Predicted direction label of the $j$ -th detection. $\mathbf{p}^j \in \mathbb{R}^{72}$
$\mathbf{P}$	Predicted direction label matrix with $\mathbf{p}^j$ rows. $\mathbf{P} \in \mathbb{R}^{\text{num of obj} \times 72}$
$\mathbf{gtd}$	Ground truth direction label vector. $\mathbf{gtd} \in \mathbb{R}^{\text{num of obj}}$
$\mathit{dir}^{(i)}$	Argmax of the predicted direction label of assigned object to $i$ -th tracklet
$\mathcal{D}^{(i)}$	Target direction stack of $i$ -th tracklet with $\mathit{dir}^{(i)}$ (one) element. $\mathcal{D}^{(i)} \in \mathbb{R}$
$\mathit{pos}^{(i)}(t)$	The position coordinate of $i$ -th tracklet at time step $t$ . $\mathit{pos}^{(i)}(t) \in \mathbb{R}^4$
$\mathbf{Pos}^{(i)}$	The position coordinates of $i$ -th tracklet with $\mathit{pos}^{(i)}(t)$ elements. $\mathbf{Pos}^{(i)} \in \mathbb{R}^{4 \times T^{(i)}}$
$\mathit{gsp}^{(i)}$	The GSP for $i$ -th tracklet
$\mathbf{b}^{(i)}$	Global embedding vector of $i$ -th tracklet, obtained by GIAOTracker
$\mathcal{B}^{(i)}$	Global embedding stack of $i$ -th tracklet with $\mathbf{b}^{(i)}$ elements
$\langle \cdot, \cdot \rangle$	Inner product
$[\cdot]$	Appending operator
$(\cdot)^T$	Matrix transpose
$\mathbf{a}$	Vector. $a_k$ is $k$ -th index of $\mathbf{a}$
$\mathbf{A}$	Matrix. $\mathbf{A}_k$ is $k$ -th row of $\mathbf{A}$
$\bar{\mathbf{A}}$	Tensor. $\bar{\mathbf{A}}_k$ is $k$ -th slice of $\bar{\mathbf{A}}$

all the training examples, we generate the JSON file with COCO format as the input. During the inference time, we pursue the feature bank approach introduced in the original DeepSORT to store clothes color information in a stack  $\mathcal{C}^{(i)}$  with a specified length  $SL^{(i)}$ . In more detail, for the  $i$ -th tracklet at time  $t \in \mathbb{SL}^{(i)}$ , we construct a stack of clothes color information  $\mathcal{C}^{(i)}(t)$  and we append the clothes color information  $\mathbf{c}^{(i)}$  of the assigned object to the  $i$ -th tracklet to its previous clothes color information stack  $\mathcal{C}^{(i)}(t-1)$ :

$$\mathcal{C}^{(i)}(t) = \text{append}[\mathcal{C}^{(i)}(t-1); \mathbf{c}^{(i)}] \quad (8)$$

**Clothes Style.** Similar to the approach taken with clothes color, we treat clothes style as another classification problem. For training, we utilize the top-20 categories from the DeepFashion dataset [56], employing a similar annotation procedure as used for the clothes color module. During the training phase, we utilize a cross-entropy loss function:

$$\mathcal{L}_{style}(\mathbf{gts}, \mathbf{s}) = - \sum_{k=1}^{20} \mathbf{gts}_k \log(s_k) + (1 - \mathbf{gts}_k) \log(1 - s_k) \quad (9)$$

where  $[\mathbf{gts}_1, \dots, \mathbf{gts}_{20}] = \mathbf{gts}$  is the label corresponding to the input of network and  $[s_1, \dots, s_{20}] = \mathbf{s}$  is the output of network from style head. In the inference time, similar to the clothes color feature bank introduced in the previous subsection, we

store clothes style information in a stack  $\mathcal{S}^{(i)}$  with a specified length  $SL^{(i)}$ . In more details, for the  $i$ -th tracklet at time  $t \in \mathbb{SL}^{(i)}$ , we construct a stack of clothes style information  $\mathcal{S}^{(i)}(t)$ , and we append the clothes style information  $\mathbf{s}^{(i)}$  of the assigned object to the  $i$ -th tracklet to its previous clothes style information stack  $\mathcal{S}^{(i)}(t-1)$ :

$$\mathcal{S}^{(i)}(t) = \text{append}[\mathcal{S}^{(i)}(t-1); \mathbf{s}^{(i)}] \quad (10)$$

**Direction.** We have chosen the MEBOW dataset [57] as our data source for orientation annotation due to its rich contextual information. The diversity of human classes captured in the MEBOW dataset, across various conditions such as different poses, lighting conditions, occlusion types, and backgrounds, makes it a suitable candidate for both developing and evaluating models for body orientation and direction estimation. Moreover, the MEBOW dataset includes annotations for orientation and body direction. In the dataset, human orientation  $\theta \in [0, 360)$  is defined and split into 72 bins. The images of subjects are fed through the YOLOX backbone, which acts as a feature extractor. The extracted features are then concatenated and processed by a few more residual layers with one fully connected layer and 72 neurons as the outputs  $\mathbf{p}$  at the end, in the direction's head. The output of each neuron,  $p_k$ , indicates the probability of the body orientation  $\theta$  being within the range of  $(5.k - 2.5, 5.k + 2.5)$ . The objective function of

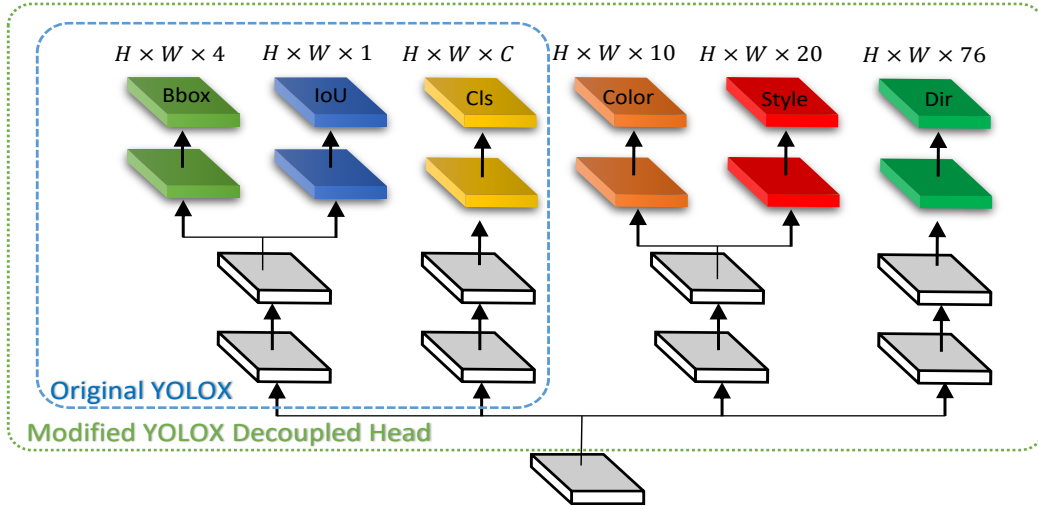


Fig. 3: Modified structure of the decoupled head of the YOLOX.

the head for direction is similar to that of MEBOW model [57], where we take inspiration from the heatmap regression idea that has been successful in key-point estimation task. We let the loss function be:

$$\mathcal{L}_{direction}(gtd, \mathbf{p}) = \sum_{k=1}^{72} (p_k - \phi(gtd, k, \sigma)) \quad (11)$$

where  $\phi(gtd, k, \sigma)$  is the circular Gaussian probability as:

$$\phi(gtd, k, \sigma) = \frac{1}{\sqrt{2\pi\sigma^2}} e^{-\frac{1}{2\sigma^2} \min(|k-gtd|, 72-|k-gtd|)^2} \quad (12)$$

and  $gtd$  is the ground-truth direction bin. In other words, equation (12) is equivalent to regressing a Gaussian function centered at the ground-truth orientation bin. Within the inference time, for the  $i$ -th tracklet we consider a stack of directional information  $\mathcal{D}^{(i)}$  with the size of 1, and in the frame  $t \in \mathbb{S}\mathbb{L}^{(i)}$ , we set the maximum index of the directional information  $\mathbf{p}^{(i)}$  of the assigned object to the  $i$ -th tracklet to its directional information stack  $\mathcal{D}^{(i)}(t)$ :

$$\{\mathcal{D}^{(i)}(t)\} \leftarrow dir^{(i)} = \operatorname{argmax}\{\mathbf{p}^{(i)}\} \quad (13)$$

**Edge-features.** The original DeepSORT uses a simple CNN ReID network to extract edge features corresponding to each object. We use a stronger appearance feature extractor, BoT [9], as our ReID network to obtain appearance embeddings. Moreover, unlike DeepSORT that exploits the feature gallery approach, we utilize Exponential Moving Average (EMA) algorithm [51] for appearance updating. Although the feature gallery approach in DeepSORT, which keeps a collection of the embedding features of an object over time, can save long-term information, it is vulnerable to detection noise [14]. To alleviate this issue, we use the feature updating strategy suggested in [51], that evolves the appearance state  $\mathbf{e}^{(i)}(t)$  for the  $i$ -th tracklet at frame  $t$  with an EMA as follows:

$$\mathbf{e}^{(i)}(t) = \alpha \mathbf{e}^{(i)}(t-1) + (1-\alpha) \mathbf{f}^{(i)}(t) \quad (14)$$

where  $\mathbf{f}^{(i)}(t)$  is the embedding of the current assigned detection to the  $i$ -th tracklet, and  $\alpha$  is a momentum term that we set to 0.8. The EMA performs a soft updating strategy for

the appearance information over time and is relatively robust with respect to detection noise. Experiments show that the EMA approach can boost the matching quality and improve the time consumption. We also update the embedding stack  $\mathcal{E}^{(i)}$  of  $i$ -th tracklet at frame  $t \in \mathbb{S}\mathbb{L}^{(i)}$  by appending the appearance state  $\mathbf{e}^{(i)}(t)$  to it:

$$\mathcal{E}^{(i)}(t) = \operatorname{append}[\mathcal{E}^{(i)}(t-1); \mathbf{e}^{(i)}] \quad (15)$$

### C. Online Tracking Algorithm

Unlike most SOTA tracker algorithms, whose acceptable performance is stipulated on offline post-processing, we focus on online tracking. Consequently, we present the majority of our results in the online scenario in the experiment section.

**Tracking Separately.** Our proposed tracker is not only suitable for pedestrian tracking but also can be deployed in the crosswalk environments, where different types of objects are of interest for tracking, e.g. cars, trucks, bikes, etc. Accordingly, we split the detected objects into separated subsets based on their object type and match each subset separately. This design choice enables us to perform hyperparameter optimization for each specific subset. Subset hyperparameter optimization is a crucial task, as there should be different settings for the Kalman parameters and matching thresholds; otherwise, the tracking performance degrades noticeably. Moreover, dividing the objects into subsets prevents the potential risk of ID switching between different object types.

**NSA Kalman.** In the online tracking framework, motion prediction is another key module. To analyze the motion information, the original Gaussian filtering (Kalman filter) is not robust with respect to imperfect detections [58] and ignores the information on scales of detection noise [14]. To address this issue, we use the same idea of NSA Kalman approach [14], which suggests an adaptive formula to derive the adaptive noise covariance  $\hat{\mathbf{R}}(t)$ :

$$\hat{\mathbf{R}}(t) = (1 - \operatorname{Conf}(t)) \mathbf{R}(t) \quad (16)$$

where  $\mathbf{R}(t)$  is the measurement noise covariance, which is usually a constant, and  $\operatorname{Conf}(t)$  is the detection confidence score at time step  $t$ . The interpretation of such a choice is that



$$\mathbf{D}_{combined} = \begin{cases} \lambda_{motion}\mathbf{D}_{motion} + \lambda_{edge}\mathbf{D}_{edge} + \lambda_{color}\mathbf{D}_{color} + \lambda_{style}\mathbf{D}_{style}, & \text{if IoU} > \text{IoU}_{min} \text{ and } \mathbf{D}_{direction} < \text{Dir}_{max} \\ d_{max} + \epsilon, & \text{otherwise.} \end{cases} \quad (20)$$

the detection has a higher score  $Conf(t)$  when it has less noise, and accordingly, has a low  $\hat{\mathbf{R}}(t)$ . Relying on equation (5), a lower  $\hat{\mathbf{R}}(t)$  means that the detection will have a higher weight in the state update step, and vice versa. This modification can enhance the overall state update procedure.

**Combined Distance.** During inference, in addition to  $\mathbf{D}_{motion}$  and  $\mathbf{D}_{edge}$ , standing for motion distance and edge feature distance introduced in previous works [13], [51], relying on our feature modules, we further introduce  $\mathbf{D}_{color}$ ,  $\mathbf{D}_{style}$  and  $\mathbf{D}_{direction}$  which are color distance, style distance and direction distance, respectively.  $\mathbf{D}_{color}(i, j)$ ,  $\mathbf{D}_{style}(i, j)$  and  $\mathbf{D}_{direction}(i, j)$  of the  $j$ -th object to the  $i$ -th tracklet at frame  $t$  are calculated as follows:

$$\mathbf{D}_{color}(i, j) = \min \left( \text{eq(7)}(\mathbf{c}^{(i)}, \mathbf{c}^j) \mid \forall \mathbf{c}^{(i)} \in \mathcal{C}^{(i)}(t) \right) \quad (17)$$

$$\mathbf{D}_{style}(i, j) = \min \left( \text{eq(9)}(\mathbf{s}^{(i)}, \mathbf{s}^j) \mid \forall \mathbf{s}^{(i)} \in \mathcal{S}^{(i)}(t) \right) \quad (18)$$

$$\mathbf{D}_{direction}(i, j) = \left( \text{eq(11)}(\mathbf{dir}^{(i)}, \mathbf{p}^j) \mid \mathbf{dir}^{(i)} \leftarrow \mathcal{D}^{(i)}(t) \right) \quad (19)$$

where,  $\mathbf{c}^j$ ,  $\mathbf{s}^j$  and  $\mathbf{p}^j$  are the outputs of the color head, style head, and direction head for the  $j$ -th object, respectively. We use Euclidean-based motion distance for  $\mathbf{D}_{motion}$  and cosine distance for  $\mathbf{D}_{edge}$  [59] as in eq.(1). We find that combining  $\mathbf{D}_{motion}$ ,  $\mathbf{D}_{edge}$ ,  $\mathbf{D}_{color}$ , and  $\mathbf{D}_{style}$  as a weighted sum with parameter  $\lambda$ , conditioned on the IoU value and  $\mathbf{D}_{direction}$  is more promising compared to the vanilla distance metric, which is a simple summation over all cost elements. Therefore, similar to [60], we introduce a *combined* distance  $\mathbf{D}_{combined}$  as in eq.(20), where  $\lambda = [\lambda_{motion}, \lambda_{edge}, \lambda_{color}, \lambda_{style}]$  is the combination weight factor,  $\text{Dir}_{max}$  is a maximum threshold for direction distance,  $\text{IoU}_{min}$  is a minimum threshold for IoU,  $d_{max}$  is a predefined high value and  $\epsilon$  is a small value like  $10^{-3}$ .

**Matching.** For subset matching, we use Hungarian matching which is a general algorithm for solving linear assignment problem. An interesting finding is that although the matching cascade algorithm is nontrivial in DeepSORT, it limits the performance as the tracker becomes more powerful. The reason is that as the tracker becomes stronger, it becomes more robust to confusing associations. Therefore, additional prior constraints limit the matching accuracy [61]. We tackle this issue by switching to the Hungarian matching, which solves a global linear assignment problem.

#### D. Post Processing

After performing the online tracking detailed in the previous section, post-processing algorithms can be applied for further modifications. For instance, a Gaussian smoothing process

can be employed to filter outliers and smooth the trajectories. Additionally, global linking algorithms can be used to merge similar trajectories as another post-processing option.

**GSP.** After matching and updating all tracklets, we conduct Gaussian smoothing process (GSP) on the trajectories of the updated tracklets to adjust recorded locations. Interpolation is commonly employed to fill gaps in trajectories caused by missing data with appropriate values. While linear interpolation is a straightforward choice due to its simplicity, it lacks precision as it doesn't incorporate motion information. Although several strategies have been suggested to tackle this issue, we present a lightweight interpolation algorithm that employs GSP to model nonlinear motion. Considering the nature of smoothing equations [20], this interpolation benefits from the information of future observations as well as past observations. This property of GSP can handle the missing problem, where the accurate correctness terms are applied to the missing points. Relying on [20], we formulate the GSP model for the  $i$ -th tracklet's trajectory as follows:

$$pos^{(i)}(t) = gsp^{(i)}(t) + \epsilon \quad (21)$$

where  $t \in \mathbb{T}^{(i)} = [1, \dots, T^{(i)}]$  is the frame ID,  $pos^{(i)}(t) \in \mathbf{Pos}^{(i)} = [pos^{(i)}(1), \dots, pos^{(i)}(T^{(i)})]$  is the position coordinate variable at frame  $t$  (i.e.,  $x, y, w, h$ ) and  $\epsilon \sim \mathcal{N}(0, \sigma^2)$  is Gaussian noise. For each tracklet and its linearly interpolated trajectory  $\mathbb{S}^{(i)} = \{t, pos^{(i)}(t)\}_{t \in \mathbb{T}^{(i)}}$  with length  $T^{(i)}$ , GSP aims to train a function  $gsp^{(i)}$  that is a Gaussian process such that it fits our data.

$$gsp^{(i)} = \text{GP}(0, k(\cdot, \cdot)) \quad (22)$$

where  $k(\cdot, \cdot)$  is a radial basis function kernel [62]. Considering the properties of the Gaussian process, for the  $i$ -th tracklet we can conduct the prediction step for the new observations in the new frame set  $\mathbb{T}^*$ , where their smoothed position  $\mathbf{Pos}^*$  is predicted by:

$$\mathbf{Pos}^* = \text{Cov}(\mathbb{T}^*, \mathbb{T}^{(i)}) (\text{Cov}(\mathbb{T}^{(i)}, \mathbb{T}^{(i)}) + \mathbf{I}\sigma^2)^{-1} \mathbf{Pos}^{(i)} \quad (23)$$

where  $\text{Cov}(\cdot, \cdot)$  is the covariance matrix.

**Global Linking.** Global link is used to predict the connectivity between two tracklets by relying only on spatiotemporal information. We use the link algorithm in GIAOTracker [14] that utilizes an improved ResNet50-TP to obtain 3D embedding corresponding to each tracklet and performs assignment with additional spatial and temporal distances. In more detail, GIAOTracker takes consecutive  $N$  frames of a tracklet clip as input and obtains features at the frame level first and outputs the clip features by temporal modeling. GIAOTracker adds part level features supervised by additional triplet loss, which enables the model to focus on detailed features of different parts of objects and be more robust to occlusion. For

TABLE II: Ablation study on the MOT17 validation set for basic strategies, i.e., stronger ReID embedding extractor (BoT), NSA Kalman filter (NSA), EMA feature updating mechanism (EMA), combined distance cost (CD) and abandoning matching cascade, i.e. vanilla matching (VM). All the results are provided in online manner without post processing. (best in bold)

Method	BoT [9]	NSA [14]	EMA [51]	CD	VM	Color	Style	Dir	MOTA↑	HOTA↑	IDF1↑	IDs↓
Vanilla Model	-	-	-	-	-	-	-	-	75	61.2	74.5	2936
FeatureSORTv1	✓	-	-	-	-	-	-	-	76.8	61.8	75.2	2840
FeatureSORTv2	✓	✓	-	-	-	-	-	-	76.9	61.8	75.4	2787
FeatureSORTv3	✓	✓	✓	-	-	-	-	-	76.8	62	75.4	2721
FeatureSORTv4	✓	✓	✓	✓	-	-	-	-	77.4	62.4	75.6	2695
FeatureSORTv5	✓	✓	✓	✓	✓	-	-	-	77.9	62.4	76	2730
FeatureSORTv6	✓	✓	✓	✓	✓	✓	-	-	79	62.8	76.9	2352
FeatureSORTv7	✓	✓	✓	✓	✓	✓	✓	-	<b>80.6</b>	<b>64.2</b>	76.7	2637
FeatureSORTv8	✓	✓	✓	✓	✓	-	-	✓	78.4	62.4	76.6	<b>1023</b>
FeatureSORTv9	✓	✓	✓	✓	✓	✓	✓	✓	79.6	63	<b>77.2</b>	2269

TABLE III: Results of applying GlobalLink and GSP to various MOT methods. All experiments are performed on the MOT17 validation set with a single GPU in an offline manner. (best in bold)

Method	GlobalLink	GSP	MOTA↑	HOTA↑	IDF1↑	IDs↓
	-	-	77.9	62.4	76	2730
FeatureSORTv5	✓	-	80.2	62.5	76	2568
	✓	✓	<b>80.4</b>	<b>62.8</b>	<b>76.4</b>	<b>2568</b>
	-	-	80.6	64.2	76.7	2637
FeatureSORTv7	✓	-	80.8	64.8	76.9	2421
	✓	✓	<b>81.2</b>	<b>65</b>	<b>76.8</b>	<b>2421</b>
	-	-	79.6	63	77.2	2269
FeatureSORTv9	✓	-	79.9	63.2	77.5	1977
	✓	✓	<b>80.2</b>	<b>63.2</b>	<b>77.7</b>	<b>1977</b>
	-	-	67.8	60.3	64.7	3039
CenterTrack [11]	✓	-	69.4	61	65	2765
	✓	✓	<b>69.7</b>	<b>61.1</b>	<b>65.3</b>	<b>2765</b>
	-	-	74.5	54.1	63.9	3663
TransTrack [2]	✓	-	74.8	54.5	64	3498
	✓	✓	<b>75</b>	<b>54.8</b>	<b>64.3</b>	<b>3498</b>
	-	-	73.7	59.3	72.3	3303
FairMOT [5]	✓	-	74.1	<b>59.6</b>	<b>72.3</b>	<b>2957</b>
	✓	✓	<b>74.4</b>	59.6	72.2	2957

temporal modeling, they use inter-frame information interaction with a Transformer encoder layer. The tracklet assignment is conducted afterward with the Hungarian matching algorithm, where the appearance cost between  $i$ -th and  $j$ -th tracklets is the smallest cosine distance between their global encoded (feature) banks  $\mathcal{B}^{(i)}$  and  $\mathcal{B}^{(j)}$  obtained by GIAOTracker:

$$C(i, j) = \min\{1 - \langle \mathbf{b}^{(i)}, \mathbf{b}^{(j)} \rangle | \forall \mathbf{b}^{(i)} \in \mathcal{B}^{(i)}, \forall \mathbf{b}^{(j)} \in \mathcal{B}^{(j)}\}. \quad (24)$$

## V. RESULTS

### A. Experimental Setup

**Datasets.** We perform experiments on the MOT16-MOT17 [10] and MOT20 [12] datasets. MOT17 is a benchmark dataset in the field of multi-object tracking, comprising 7 sequences with 5,316 frames for training and 7 sequences with 5919 frames for testing. MOT20, another benchmark dataset, covers highly crowded and challenging pedestrian views, with 4 sequences and 8,931 frames for training and 4 sequences and 4,479 frames for testing. Similar to previous works [63],

[64], we use the first half of each sequence in the MOT16, MOT17 and MOT20 training sets for training and the last half for validation. We train the detector using the CrowdHuman dataset [54] and half of the training sets from MOT16, MOT17, and MOT20 for ablation, as outlined in [52], [53]. Additionally, we include ETHZ [55] for testing, following the methodology in [52], [53].

**Metrics.** We assess various aspects of tracking performance using CLEAR metrics [6], which include MOTA, FP, FN, and IDs, along with HOTA [7] and IDF1 [65]. MOTA provides an overall tracking accuracy, IDF1 measures the algorithm’s association ability, and HOTA, which is a newer metric proposed in [7], balances the effect of accurate detection, association, and localization.

**Implementation Details.** We provide the overall information related to the implementation of our algorithm in this section. We use YOLOX for an improved time-accuracy trade-off, adapting its structure to provide style, color, and direction information in addition to bounding boxes and class probabilities. Our training schedule and settings for the



TABLE IV: Ablation study on the MOT17 validation set for the matching cascade algorithm and vanilla matching. All the results are in online mode without post processing. (best in bold)

Method	Matching	MOTA $\uparrow$	HOTA $\uparrow$	IDF1 $\uparrow$	IDs $\downarrow$
DeepSORT	cascade	77.3	60.5	76	3374
	vanilla	76.2	60.4	76	3416
FeatureSORTv5	cascade	77.7	62.4	76	2769
	vanilla	77.9	62.4	76	2730
FeatureSORTv6	cascade	79	62.7	76.6	2412
	vanilla	79	62.8	76.9	2352
FeatureSORTv7	cascade	80.5	64	76.6	2613
	vanilla	<b>80.6</b>	<b>64.2</b>	76.7	2637
FeatureSORTv8	cascade	78.2	62.4	76.5	1098
	vanilla	78.4	62.4	76.6	<b>1023</b>
FeatureSORTv9	cascade	79.5	63	77.2	2293
	vanilla	79.6	63	<b>77.2</b>	2269

classification and localization heads of the detector are similar to those optimal configuration used in previous works [13], [61]. For the feature heads (color, style, and direction), we freeze the entire network’s weights except for the feature heads and train the detector for an additional 50 epochs utilizing scheduled learning rate with exponential decay optimized by grid search. During inference, we set the thresholds for non-maximum suppression (NMS) and detection confidence at 0.8 and 0.5, respectively. The IoU value threshold for matching is 0.45, the momentum term ( $\alpha$ ) in EMA is 0.8, and the weight factors for distance,  $\lambda = [\lambda_{motion}, \lambda_{edge}, \lambda_{color}, \lambda_{style}]$ , are set as follows: 0.1 for motion, 0.4 for edge, 0.25 for color, and 0.25 for style.  $Age_{max}$  is set to 10 frames to delete the tracklets which are not updated for the periods more than this threshold. The maximum gap allowed for interpolation in GSP is 20 frames. In addition to the MARS ReID dataset [48], for Global Linking, we utilize a car ReID dataset created by GIAOTracker. The input size of the global linking network is set to [224, 224, 4] for vehicle tracklet clips and [224, 112, 4] for pedestrian tracklets. We utilize Adam as the optimizer and cross-entropy loss as the objective function for training the global linking network over 50 epochs, employing a learning rate schedule of cosine annealing. During inference, we apply a temporal distance threshold of 20 frames and a spatial distance threshold of 70 pixels to remove unrealistic association pairs. Finally, the association is accepted if its score predicted by the network is larger than 0.9. All experiments are conducted on an NVIDIA RTX 4060 8GB GPU.

### B. Ablation Studies

We divide our ablation studies into three parts. First, we examine how our feature-based modules introduced in section IV-B affect overall tracking performance. Second, we demonstrate the necessity of post-processing by evaluating GSP and Global Linking. Finally, we compare our proposed vanilla matching with the cascade matching in DeepSORT [3] to show the effectiveness of the suggested matching algorithm.

**Ablation study for feature-based modules.** In table II we detail the enhancements we applied to DeepSORT to create FeatureSORT and empirically demonstrates the effectiveness of these applied modules.

- 1) BoT: Replacing the original ReID embedding extractor with BoT results in a MOTA improvement of +1.8 and IDF1 of +0.7, indicating that association quality relies on discriminative appearance features.
- 2) NSA: The NSA Kalman filter further enhances MOTA by +0.1 and IDF1 by 0.2+. This means that it improves positioning accuracy as it modifies motion update equations.
- 3) EMA: The EMA feature updating mechanism provides the ability of better association (+0.2 HOTA).
- 4) CD: Matching incorporating feature-based modules distances and motion distance as described in IV-B, aids association MOTA (+0.6) and IDF1 (+0.2) and HOTA (+0.4). In FeatureSORTv4 we only used motion, edge and IoU distances in equation (20).
- 5) VM: By simply utilizing a vanilla matching method, IDF1 is improved (+0.4) and MOTA (+0.5). We also use cascade matching for the sake of comparison.
- 6) Color: By employing color features and including them in the cost function, we have witnessed a relatively significant improvement in MOTA (+1.1), while IDF1 is also improved (+0.9). In figure 4, an example is provided in which utilizing the color module prevents wrong ID matching. In the left three consecutive frames without color distance in cost function (20), an ID switch occurs for ID number 35. However, by incorporating color distance in 20, the issue is resolved in the right three images.
- 7) Style: Similar to color features, by integrating style features in the cost function, we obtain an increase in both MOTA (+1.6) and HOTA(+1.4), while IDs increased since highly detailed features lead to not matching and assigning new ID to the objects.
- 8) Direction: As directional features provide the direction of movements of the objects, considering it in the cost function in equation (20) results in a significant drop in the IDs. Figure 5 provides an example, where exploiting the direction module prevents the ID switch. In the left three consecutive frames without direction distance in cost function (20), an ID switch occurs for ID number 23. By incorporating direction distance in 20, the issue is resolved in the right three images.

**Ablation study for Global Linking and GSP.** We apply Global Linking and GSP on six different tracking algorithms, three versions of FeatureSORT and three state-of-the-art trackers (CenterTrack [11], TransTrack [2] and FairMOT [5]). Their results are shown in Table III. The first row of the results for each tracking algorithm is the baseline performance in which we use neither Global Linking nor GSP. Depending on the type of tracking algorithm, incorporating Global Linking (the second row) provides different levels of enhancements. Particularly, trackers with poorer performance benefit more from Global Linking since they are more prone to missing associations. The third row of the table for each tracker shows the merit of using GSP for different evaluating metrics. GSP works better on stronger trackers, but it cannot provide reliable results for the weaker trackers due to the large amount of false



Fig. 4: Color module effect.

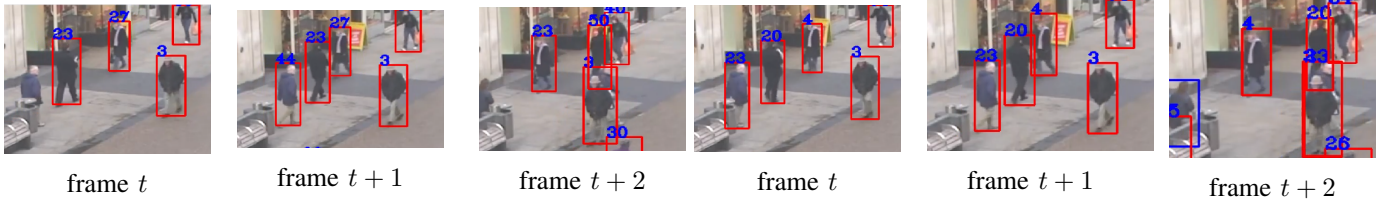


Fig. 5: Direction module effect.

TABLE V: Comparison of FeatureSORT and DeepSORT using light (modified) YOLOX models on the MOT17 validation set.

Detector	Params	Tracker	MOTA $\uparrow$	HOTA $\uparrow$	IDF1 $\uparrow$	IDs $\downarrow$
YOLOX-L	61M	FeatureSORTv9	77.8	61.8	76.3	157
		DeepSORT	75.6	59.9	73	169
YOLOX-M	28M	FeatureSORTv9	76.3	60.4	74.6	177
		DeepSORT	74.5	59.1	76.9	197
YOLOX-S	10.5M	FeatureSORTv9	72.6	58.7	73.9	183
		DeepSORT	69.6	56	71.5	205
YOLOX-Tiny	5.8M	FeatureSORTv9	72.4	57.9	73.3	194
		DeepSORT	68.6	54.6	72	224
YOLOX-Nano	1M	FeatureSORTv9	65.9	52.3	69.1	173
		DeepSORT	61.4	49	66.8	161

associations.

**Ablation study for vanilla matching.** Table IV compares the matching cascade algorithm and vanilla matching on different versions of FeatureSORT. Based on the results of table IV, the matching cascade algorithm provides better results for DeepSORT. However, it has considerably smaller improvement over FeatureSORT versions and is even harmful to some versions with respect to tracking accuracy. Considering the results of table IV, we can conclude that while the prior assumption in the matching cascade can reduce confusing associations in weaker trackers, it imposes significant constraints on stronger trackers and limits their performance [13].

**Tracking performance of light modified YOLOX.** We compare FeatureSORT and DeepSORT using light detection models. FeatureSORT utilizes our modified version of YOLOX with four heads, while DeepSORT employs the original YOLOX structure with two heads. All models are trained on a combination of the MOT17, COCO and CrowdHuman datasets. The input image size is set to  $(1088 \times 608)$ , with the shortest side varying from 384 to 832 during multi-scale training. The results are presented in Table V. Thanks to the integrated feature modules, FeatureSORT consistently improves upon MOTA,

HOTA, and IDF1. Remarkably, when employing the lightweight YOLOX-Nano as the detector, FeatureSORT achieves a MOTA that is 4.5 points higher than that of DeepSORT. This makes it notably more suitable for real-world applications.

### C. Benchmark Evaluation

We submit our results to the MOT16-17-20 Challenge test server and compare them with the recent state-of-the-art online MOT models.

#### MOT16 and MOT17.

The performance of FeatureSORT in online mode without post-processing, along with its comparison with benchmarks on the MOT16 and MOT17 test sets, is provided in Tables VI and VII respectively. FeatureSORT achieves a higher MOTA on the MOT16 dataset compared to SGT [71], FairMOT [5], and StrongSORT [13] by approximately 3%, 5%, and 2%, respectively. Additionally, on the MOT17 dataset, FeatureSORT outperforms these same state-of-the-art methods by around 4%, 7%, and 2% in terms of MOTA, noting that FairMOT is trained with additional training datasets. By optionally excluding the BoT network for ReID embedding extraction in FeatureSORT,

TABLE VI: MOT16

Method	MOTA $\uparrow$	HOTA $\uparrow$	IDF1 $\uparrow$	FP $\downarrow$	FN $\downarrow$	IDs $\downarrow$
QDTrack [66]	69.8	54.5	67.1	9861	44050	1097
TraDes [52]	70.1	53.2	64.7	<b>8091</b>	45210	1144
CSTrack [50]	75.6	59.8	73.3	9646	33777	1121
GSDT [67]	74.5	56.6	68.1	8913	36428	1229
RelationTrack [68]	75.6	61.7	75.8	9786	34214	<b>448</b>
OMC [69]	76.4	62.9	74.1	10821	31044	1087
CorrTracker [70]	76.6	61.0	74.3	10860	30756	979
SGT [71]	76.8	61.2	73.5	10695	30394	1276
FairMOT [5]	74.9	58.3	72.8	9952	38451	1074
StrongSORT [13]	77.8	63.8	<b>78.3</b>	11254	32584	1538
FeatureSORTv7	<b>79.7</b>	<b>63.8</b>	76.6	9182	27563	1658
FeatureSORTv8	77.9	62.8	76.3	14827	26877	597
FeatureSORTv9	78.3	63.1	76.8	13321	<b>24992</b>	1336

TABLE VII: MOT17

Method	MOTA $\uparrow$	HOTA $\uparrow$	IDF1 $\uparrow$	FP $\downarrow$	FN $\downarrow$	IDs $\downarrow$
CTracker [72]	66.6	49.0	57.4	22284	160491	5529
CenterTrack [11]	67.8	60.3	64.7	<b>18489</b>	160332	3039
QDTrack [66]	68.7	63.5	66.3	26598	146643	3378
TraDes [52]	69.1	52.7	63.9	20892	150060	3555
SOTMOT [73]	71	64.1	71.9	39537	118983	5184
GSDT [67]	73.2	55.2	66.5	26397	120666	3891
RelationTrack [68]	73.8	59.9	74.7	27999	118623	1374
TransTrack [2]	74.5	54.1	63.9	28323	112137	3663
OMC-F [69]	74.7	56.8	73.8	30162	108556	-
CSTrack [50]	74.9	59.3	72.3	23847	114303	3567
OMC [69]	76	57.1	73.8	28894	101022	-
SGT [71]	76.3	57.3	72.8	25974	102885	4101
CorrTracker [70]	76.4	58.4	73.6	29808	99510	3369
FairMOT [5]	73.7	59.3	72.3	27507	117477	3303
DeepSORT [3]	78	61.2	74.5	29852	94716	1821
ByteTrack [61]	78.9	62.8	77.2	25491	83721	2196
StrongSORT [13]	78.3	63.5	<b>78.5</b>	27876	86205	1446
FeatureSORTv7	<b>80.6</b>	<b>64.2</b>	76.7	27581	84362	2637
FeatureSORTv8	78.4	62.4	76.6	30294	87928	<b>1023</b>
FeatureSORTv9	79.6	63	77.2	29588	<b>83132</b>	2269

we can consider FeatureSORT as a joint detector-tracker. This makes it a viable candidate for comparison with FairMOT when the edge distance provided by the BoT network is removed from the cost function. FeatureSORTv9 achieves high MOTA, HOTA, and IDF1 on MOT16-17 based on the optimal trade-off between FP, FN, and IDs.

When compared to models utilizing the same detector, such as StrongSORT and ByteTrack [61], FeatureSORT outperforms them across most MOT metrics. Furthermore, in comparison to OMC-F [69], which is tailored for tracking low-scored detections, FeatureSORT exhibits superior performance in terms of MOTA, HOTA, IDF1, and shows fewer false negatives and false positives, highlighting the superiority of our mechanism over OMC.

**MOT20.** MOT20, a newer challenge released after MOT16-17, encompasses scenes of severe crowding and prevalent partial occlusion. Employing the same detection threshold, existing methods face missed detections due to less confident output. Some works like [5], [70] opt for a lower detection threshold for MOT20; however, this leads to high FP, IDs, and low IDF1, as their pairwise relational features struggle with accurately matching a large number of tracking candidates. Conversely, using feature-based modules and, accordingly, higher-order relational features, FeatureSORT effectively addresses this issue, achieving state-of-the-art MOTA as shown in Table VIII. FeatureSORTv7 surpasses CorrTracker [70] in MOTA by 12% and shows higher MOTA than SGT by approximately 13%. FeatureSORTv9 presents a

TABLE VIII: MOT20

Method	MOTA $\uparrow$	HOTA $\uparrow$	IDF1 $\uparrow$	FP $\downarrow$	FN $\downarrow$	IDs $\downarrow$
SORT [21]	42.7	36.1	45.1	28398	287582	4852
Tracktor++ [74]	52.6	42.1	52.7	35536	236680	1648
CSTrack [50]	66.6	54	68.6	25404	144358	3196
CrowdTrack [75]	70.7	55	68.2	21928	126533	3198
RelationTrack [68]	67.2	56.5	70.5	61134	104597	4243
DeepSORT [3]	71.8	57.1	69.6	37858	101581	3754
TransTrack [2]	64.5	48.9	59.2	28566	151377	3565
CorrTracker [70]	65.2	57.1	69.1	79429	95855	5193
GSDT [67]	67.1	53.6	67.5	31913	135409	3131
SOTMOT [73]	68.6	55.7	71.4	57064	101154	4209
OMC [69]	73.1	60.5	74.4	<b>16159</b>	108654	779
FairMOT [5]	61.8	54.6	67.3	103404	88901	5243
SGT [71]	64.5	56.9	62.7	67352	111201	4909
ByteTrack [61]	75.7	60.9	74.9	26249	<b>87594</b>	1223
StrongSORT [13]	72.2	61.5	<b>75.9</b>	16632	117920	770
FeatureSORTv7	<b>77.9</b>	<b>63.4</b>	75	26223	89050	1794
FeatureSORTv8	76	61.1	74.7	27541	99582	<b>693</b>
FeatureSORTv9	76.6	61.3	75.1	25083	95027	1081

better tradeoff between FN and FP, IDs, and higher MOTA and HOTA than OMC, StrongSORT, and ByteTrack. Although OMC utilizes past frames as temporal cues to carefully select low-scored detections, its matching process remains constrained by pairwise relational features. In contrast, FeatureSORT employs vanilla matching, mitigating the limitations imposed by other complex matching algorithms, thereby outperforming OMC. By applying directional information in the cost function, FeatureSORTv8 significantly reduces IDs by preventing ID switches among crossing pedestrians, especially in crowded scenes. However, exploiting directional information limits MOTA and IDF1 scores as it ensures track IDs remain consistent and unchanged during inference.

#### D. Qualitative Results

The visualization of our tracking algorithm on the test sets of MOT16, MOT17, and MOT20 is illustrated in Figure 6. Results for MOT16-03 and MOT17-01 demonstrate the efficacy of our approach in standard scenarios. From the results of MOT17-08, correct associations post-occlusion are evident, attributed to exploiting color and style features for consistent track IDs. Results for MOT17-14 indicate that even in scenarios with camera movement, FeatureSORT maintains acceptable performance. Demonstrations for MOT20-03 and MOT20-05 highlight FeatureSORT’s robust performance in extremely crowded situations.

## VI. DISCUSSION

A primary concern regarding DeepSORT-like paradigms is their execution speed due to the requirement for ReID features. This limitation arises from the use of separate ReID networks alongside the detector module, leading to decreased processing speed. Although our results are based on using a separate ReID network for edge embedding extraction, FeatureSORT is capable of achieving commendable tracking performance even without exploiting a ReID network. This is due to modifications made to the structure of the detector, enabling the use of features obtained directly from the detector for tracking. Such an approach makes FeatureSORT similar to joint detection-tracking algorithms. It is worth noting that the features obtained from the modified YOLOX detector



in our study may not be as explicit compared to those obtained from separate networks specifically designed for tasks such as color classification, style classification, and direction classification. However, this strategy introduces a trade-off between computational complexity, processing speed, and tracking performance, necessitating a balance between these factors.

## VII. CONCLUSION

This paper enhances the classic tracker DeepSORT by integrating feature-based modules and advanced inference techniques. The resulting tracker, named FeatureSORT, represents a robust new baseline for both joint detection-tracking and tracking-by-detection models in the MOT task. Two post-processing algorithms, Global Linking and GSP, are employed to address missing association and detection issues, thereby enhancing the accuracy of trajectories. By integrating Global

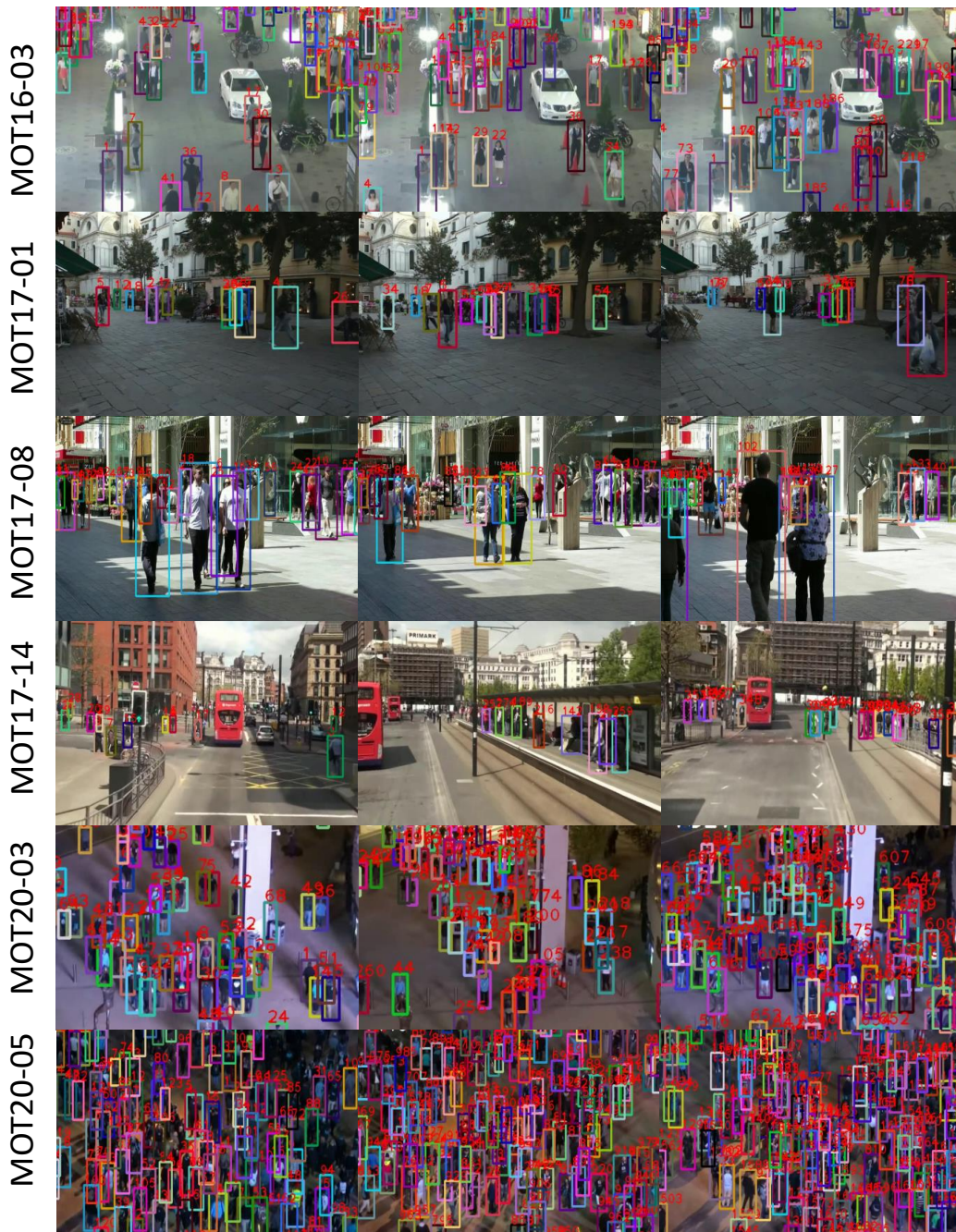


Fig. 6: Sample tracking results visualization of FeatureSORT on the test sets of MOT16, MOT17 and MOT20.

Linking and GSP into FeatureSORT, the resulting tracker achieves state-of-the-art performance on multiple benchmarks, including MOT16, MOT17, and MOT20, in offline mode.

## REFERENCES

- [1] A. Milan, S. Roth, and K. Schindler, "Continuous energy minimization for multitarget tracking," *IEEE transactions on pattern analysis and machine intelligence*, vol. 36, no. 1, pp. 58–72, 2013.
- [2] P. Sun, J. Cao, Y. Jiang, R. Zhang, E. Xie, Z. Yuan, C. Wang, and P. Luo, "Transtrack: Multiple object tracking with transformer," *arXiv preprint arXiv:2012.15460*, 2020.
- [3] N. Wojke, A. Bewley, and D. Paulus, "Simple online and realtime tracking with a deep association metric," in *2017 IEEE international conference on image processing (ICIP)*. IEEE, 2017, pp. 3645–3649.
- [4] Y. Xiang, A. Alahi, and S. Savarese, "Learning to track: Online multi-object tracking by decision making," in *Proceedings of the IEEE international conference on computer vision*, 2015, pp. 4705–4713.
- [5] Y. Zhang, C. Wang, X. Wang, W. Zeng, and W. Liu, "Fairmot: On the fairness of detection and re-identification in multiple object tracking," *International Journal of Computer Vision*, vol. 129, pp. 3069–3087, 2021.
- [6] K. Bernardin and R. Stiefelhagen, "Evaluating multiple object tracking performance: the clear mot metrics," *EURASIP Journal on Image and Video Processing*, vol. 2008, pp. 1–10, 2008.
- [7] J. Luiten, A. Osep, P. Dendorfer, P. Torr, A. Geiger, L. Leal-Taixé, and B. Leibe, "Hota: A higher order metric for evaluating multi-object tracking," *International journal of computer vision*, vol. 129, pp. 548–578, 2021.
- [8] Z. Lu, V. Rathod, R. Votel, and J. Huang, "Retinatrack: Online single stage joint detection and tracking," in *Proceedings of the IEEE/CVF conference on computer vision and pattern recognition*, 2020, pp. 14 668–14 678.
- [9] H. Luo, W. Jiang, Y. Gu, F. Liu, X. Liao, S. Lai, and J. Gu, "A strong baseline and batch normalization neck for deep person re-identification," *IEEE Transactions on Multimedia*, vol. 22, no. 10, pp. 2597–2609, 2019.
- [10] A. Milan, L. Leal-Taixé, I. Reid, S. Roth, and K. Schindler, "Mot16: A benchmark for multi-object tracking," *arXiv preprint arXiv:1603.00831*, 2016.
- [11] X. Zhou, V. Koltun, and P. Krähenbühl, "Tracking objects as points," in *European conference on computer vision*. Springer, 2020, pp. 474–490.
- [12] P. Dendorfer, H. Rezatofghi, A. Milan, J. Shi, D. Cremers, I. Reid, S. Roth, K. Schindler, and L. Leal-Taixé, "Mot20: A benchmark for multi object tracking in crowded scenes," *arXiv preprint arXiv:2003.09003*, 2020.
- [13] Y. Du, Z. Zhao, Y. Song, Y. Zhao, F. Su, T. Gong, and H. Meng, "Strong-sort: Make deepsort great again," *IEEE Transactions on Multimedia*, 2023.
- [14] Y. Du, J. Wan, Y. Zhao, B. Zhang, Z. Tong, and J. Dong, "Giaotracker: A comprehensive framework for mcmot with global information and optimizing strategies in visdrone 2021," in *Proceedings of the IEEE/CVF International conference on computer vision*, 2021, pp. 2809–2819.
- [15] J. Gao and R. Nevatia, "Revisiting temporal modeling for video-based person reid," *arXiv preprint arXiv:1805.02104*, 2018.
- [16] A. A. Perera, C. Srinivas, A. Hoogs, G. Brooksby, and W. Hu, "Multi-object tracking through simultaneous long occlusions and split-merge conditions," in *2006 IEEE Computer Society Conference on Computer Vision and Pattern Recognition (CVPR'06)*, vol. 1. IEEE, 2006, pp. 666–673.
- [17] M. Hofmann, M. Haag, and G. Rigoll, "Unified hierarchical multi-object tracking using global data association," in *2013 IEEE International Workshop on Performance Evaluation of Tracking and Surveillance (PETS)*. IEEE, 2013, pp. 22–28.
- [18] B. Pang, Y. Li, Y. Zhang, M. Li, and C. Lu, "Tubetk: Adopting tubes to track multi-object in a one-step training model," in *Proceedings of the IEEE/CVF conference on computer vision and pattern recognition*, 2020, pp. 6308–6318.
- [19] H. Possegger, T. Mauthner, P. M. Roth, and H. Bischof, "Occlusion geodesics for online multi-object tracking," in *proceedings of the IEEE Conference on Computer Vision and Pattern Recognition*, 2014, pp. 1306–1313.
- [20] E. Schulz, M. Speekenbrink, and A. Krause, "A tutorial on gaussian process regression: Modelling, exploring, and exploiting functions," *Journal of Mathematical Psychology*, vol. 85, pp. 1–16, 2018.
- [21] A. Bewley, Z. Ge, L. Ott, F. Ramos, and B. Upcroft, "Simple online and realtime tracking," in *2016 IEEE international conference on image processing (ICIP)*. IEEE, 2016, pp. 3464–3468.
- [22] R. E. Kalman, "A new approach to linear filtering and prediction problems," 1960.
- [23] E. Bochinski, V. Eiselein, and T. Sikora, "High-speed tracking-by-detection without using image information," in *2017 14th IEEE international conference on advanced video and signal based surveillance (AVSS)*. IEEE, 2017, pp. 1–6.
- [24] J. Zhu, H. Yang, N. Liu, M. Kim, W. Zhang, and M.-H. Yang, "Online multi-object tracking with dual matching attention networks," in *Proceedings of the European conference on computer vision (ECCV)*, 2018, pp. 366–382.
- [25] P. Chu and H. Ling, "Famnet: Joint learning of feature, affinity and multi-dimensional assignment for online multiple object tracking," in *Proceedings of the IEEE/CVF International Conference on Computer Vision*, 2019, pp. 6172–6181.
- [26] P. Chu, H. Fan, C. C. Tan, and H. Ling, "Online multi-object tracking with instance-aware tracker and dynamic model refreshment," in *2019 IEEE winter conference on applications of computer vision (WACV)*. IEEE, 2019, pp. 161–170.
- [27] Y. Zhang, H. Sheng, Y. Wu, S. Wang, W. Lyu, W. Ke, and Z. Xiong, "Long-term tracking with deep tracklet association," *IEEE Transactions on Image Processing*, vol. 29, pp. 6694–6706, 2020.
- [28] S. Han, P. Huang, H. Wang, E. Yu, D. Liu, and X. Pan, "Mat: Motion-aware multi-object tracking," *Neurocomputing*, vol. 476, pp. 75–86, 2022.
- [29] C. Dicle, O. I. Camps, and M. Szañier, "The way they move: Tracking multiple targets with similar appearance," in *Proceedings of the IEEE international conference on computer vision*, 2013, pp. 2304–2311.
- [30] F. Yu, W. Li, Q. Li, Y. Liu, X. Shi, and J. Yan, "Poi: Multiple object tracking with high performance detection and appearance feature," in *Computer Vision–ECCV 2016 Workshops: Amsterdam, The Netherlands, October 8–10 and 15–16, 2016, Proceedings, Part II 14*. Springer, 2016, pp. 36–42.
- [31] N. Mahmoudi, S. M. Ahadi, and M. Rahmati, "Multi-target tracking using cnn-based features: Cnnmtt," *Multimedia Tools and Applications*, vol. 78, pp. 7077–7096, 2019.
- [32] Z. Zhou, J. Xing, M. Zhang, and W. Hu, "Online multi-target tracking with tensor-based high-order graph matching," in *2018 24th International Conference on Pattern Recognition (ICPR)*. IEEE, 2018, pp. 1809–1814.
- [33] L. Zheng, H. Zhang, S. Sun, M. Chandraker, Y. Yang, and Q. Tian, "Person re-identification in the wild," in *Proceedings of the IEEE conference on computer vision and pattern recognition*, 2017, pp. 1367–1376.
- [34] A. Hermans, L. Beyer, and B. Leibe, "In defense of the triplet loss for person re-identification," *arXiv preprint arXiv:1703.07737*, 2017.
- [35] H. Luo, Y. Gu, X. Liao, S. Lai, and W. Jiang, "Bag of tricks and a strong baseline for deep person re-identification," in *Proceedings of the IEEE/CVF conference on computer vision and pattern recognition workshops*, 2019, pp. 0–0.
- [36] S.-H. Bae and K.-J. Yoon, "Robust online multi-object tracking based on tracklet confidence and online discriminative appearance learning," in *Proceedings of the IEEE conference on computer vision and pattern recognition*, 2014, pp. 1218–1225.
- [37] S. Tang, M. Andriluka, B. Andres, and B. Schiele, "Multiple people tracking by lifted multicut and person re-identification," in *Proceedings of the IEEE conference on computer vision and pattern recognition*, 2017, pp. 3539–3548.
- [38] A. Sadeghian, A. Alahi, and S. Savarese, "Tracking the untrackable: Learning to track multiple cues with long-term dependencies," in *Proceedings of the IEEE international conference on computer vision*, 2017, pp. 300–311.
- [39] L. Chen, H. Ai, Z. Zhuang, and C. Shang, "Real-time multiple people tracking with deeply learned candidate selection and person re-identification," in *2018 IEEE international conference on multimedia and expo (ICME)*. IEEE, 2018, pp. 1–6.
- [40] K. Fang, Y. Xiang, X. Li, and S. Savarese, "Recurrent autoregressive networks for online multi-object tracking," in *2018 IEEE Winter Conference on Applications of Computer Vision (WACV)*. IEEE, 2018, pp. 466–475.
- [41] L. Zhang, Y. Li, and R. Nevatia, "Global data association for multi-object tracking using network flows," in *2008 IEEE conference on computer vision and pattern recognition*. IEEE, 2008, pp. 1–8.
- [42] L. Wen, W. Li, J. Yan, Z. Lei, D. Yi, and S. Z. Li, "Multiple target tracking based on undirected hierarchical relation hypergraph," in *Proceedings of the IEEE conference on computer vision and pattern recognition*, 2014, pp. 1282–1289.
- [43] J. Berclaz, F. Fleuret, E. Turetken, and P. Fua, "Multiple object tracking using k-shortest paths optimization," *IEEE transactions on pattern analysis and machine intelligence*, vol. 33, no. 9, pp. 1806–1819, 2011.

- [44] A. Roshan Zamir, A. Dehghan, and M. Shah, "Gmcp-tracker: Global multi-object tracking using generalized minimum clique graphs," in *Computer Vision—ECCV 2012: 12th European Conference on Computer Vision, Florence, Italy, October 7–13, 2012, Proceedings, Part II 12*. Springer, 2012, pp. 343–356.
- [45] W. Choi, "Near-online multi-target tracking with aggregated local flow descriptor," in *Proceedings of the IEEE international conference on computer vision*, 2015, pp. 3029–3037.
- [46] G. Brasó and L. Leal-Taixé, "Learning a neural solver for multiple object tracking," in *Proceedings of the IEEE/CVF conference on computer vision and pattern recognition*, 2020, pp. 6247–6257.
- [47] A. Hornakova, R. Henschel, B. Rosenhahn, and P. Swoboda, "Lifted disjoint paths with application in multiple object tracking," in *International Conference on Machine Learning*. PMLR, 2020, pp. 4364–4375.
- [48] MARS: A Video Benchmark for Large-Scale Person Re-identification. Springer, 2016.
- [49] Z. Ge, S. Liu, F. Wang, Z. Li, and J. Sun, "Yolox: Exceeding yolo series in 2021," *arXiv preprint arXiv:2107.08430*, 2021.
- [50] C. Liang, Z. Zhang, X. Zhou, B. Li, S. Zhu, and W. Hu, "Rethinking the competition between detection and reid in multiobject tracking," *IEEE Transactions on Image Processing*, vol. 31, pp. 3182–3196, 2022.
- [51] Z. Wang, L. Zheng, Y. Liu, Y. Li, and S. Wang, "Towards real-time multi-object tracking," in *European Conference on Computer Vision*. Springer, 2020, pp. 107–122.
- [52] J. Wu, J. Cao, L. Song, Y. Wang, M. Yang, and J. Yuan, "Track to detect and segment: An online multi-object tracker," in *Proceedings of the IEEE/CVF conference on computer vision and pattern recognition*, 2021, pp. 12 352–12 361.
- [53] F. Zeng, B. Dong, Y. Zhang, T. Wang, X. Zhang, and Y. Wei, "Motr: End-to-end multiple-object tracking with transformer," in *European Conference on Computer Vision*. Springer, 2022, pp. 659–675.
- [54] S. Shao, Z. Zhao, B. Li, T. Xiao, G. Yu, X. Zhang, and J. Sun, "Crowdhuman: A benchmark for detecting human in a crowd," *arXiv preprint arXiv:1805.00123*, 2018.
- [55] A. Ess, B. Leibe, K. Schindler, and L. Van Gool, "A mobile vision system for robust multi-person tracking," in *2008 IEEE Conference on Computer Vision and Pattern Recognition*. IEEE, 2008, pp. 1–8.
- [56] Z. Liu, P. Luo, S. Qiu, X. Wang, and X. Tang, "Deepfashion: Powering robust clothes recognition and retrieval with rich annotations," in *Proceedings of the IEEE conference on computer vision and pattern recognition*, 2016, pp. 1096–1104.
- [57] C. Wu, Y. Chen, J. Luo, C.-C. Su, A. Dawane, B. Hanzra, Z. Deng, B. Liu, J. Z. Wang, and C.-h. Kuo, "Mebow: Monocular estimation of body orientation in the wild," in *Proceedings of the IEEE/CVF Conference on Computer Vision and Pattern Recognition*, 2020, pp. 3451–3461.
- [58] D. Stadler and J. Beyerer, "Modelling ambiguous assignments for multi-person tracking in crowds," in *Proceedings of the IEEE/CVF Winter Conference on Applications of Computer Vision*, 2022, pp. 133–142.
- [59] N. Aharon, R. Orfaig, and B.-Z. Bobrovsky, "Bot-sort: Robust associations multi-pedestrian tracking," *arXiv preprint arXiv:2206.14651*, 2022.
- [60] D. Stadler and J. Beyerer, "An improved association pipeline for multi-person tracking," in *Proceedings of the IEEE/CVF Conference on Computer Vision and Pattern Recognition*, 2023, pp. 3169–3178.
- [61] Y. Zhang, P. Sun, Y. Jiang, D. Yu, F. Weng, Z. Yuan, P. Luo, W. Liu, and X. Wang, "Bytetrack: Multi-object tracking by associating every detection box," in *European Conference on Computer Vision*. Springer, 2022, pp. 1–21.
- [62] B. Scholkopf, K.-K. Sung, C. J. Burges, F. Girosi, P. Niyogi, T. Poggio, and V. Vapnik, "Comparing support vector machines with gaussian kernels to radial basis function classifiers," *IEEE transactions on Signal Processing*, vol. 45, no. 11, pp. 2758–2765, 1997.
- [63] P. Tokmakov, J. Li, W. Burgard, and A. Gaidon, "Learning to track with object permanence," in *Proceedings of the IEEE/CVF International Conference on Computer Vision*, 2021, pp. 10 860–10 869.
- [64] W. Wang, E. Xie, X. Li, D.-P. Fan, K. Song, D. Liang, T. Lu, P. Luo, and L. Shao, "Pyramid vision transformer: A versatile backbone for dense prediction without convolutions," in *Proceedings of the IEEE/CVF international conference on computer vision*, 2021, pp. 568–578.
- [65] E. Ristani, F. Solera, R. Zou, R. Cucchiara, and C. Tomasi, "Performance measures and a data set for multi-target, multi-camera tracking," in *European conference on computer vision*. Springer, 2016, pp. 17–35.
- [66] J. Pang, L. Qiu, X. Li, H. Chen, Q. Li, T. Darrell, and F. Yu, "Quasi-dense similarity learning for multiple object tracking," in *Proceedings of the IEEE/CVF conference on computer vision and pattern recognition*, 2021, pp. 164–173.
- [67] Y. Wang, K. Kitani, and X. Weng, "Joint object detection and multi-object tracking with graph neural networks," in *2021 IEEE International Conference on Robotics and Automation (ICRA)*. IEEE, 2021, pp. 13 708–13 715.
- [68] E. Yu, Z. Li, S. Han, and H. Wang, "Relationtrack: Relation-aware multiple object tracking with decoupled representation," *IEEE Transactions on Multimedia*, 2022.
- [69] C. Liang, Z. Zhang, X. Zhou, B. Li, and W. Hu, "One more check: making "fake background" be tracked again," in *Proceedings of the AAAI Conference on Artificial Intelligence*, vol. 36, no. 2, 2022, pp. 1546–1554.
- [70] Q. Wang, Y. Zheng, P. Pan, and Y. Xu, "Multiple object tracking with correlation learning," in *Proceedings of the IEEE/CVF Conference on Computer Vision and Pattern Recognition*, 2021, pp. 3876–3886.
- [71] J. Hyun, M. Kang, D. Wee, and D. Yeung, "Detection recovery in online multi-object tracking with sparse graph tracker. arxiv 2022," *arXiv preprint arXiv:2205.00968*.
- [72] J. Peng, C. Wang, F. Wan, Y. Wu, Y. Wang, Y. Tai, C. Wang, J. Li, F. Huang, and Y. Fu, "Chained-tracker: Chaining paired attentive regression results for end-to-end joint multiple-object detection and tracking," in *Computer Vision—ECCV 2020: 16th European Conference, Glasgow, UK, August 23–28, 2020, Proceedings, Part IV 16*. Springer, 2020, pp. 145–161.
- [73] L. Zheng, M. Tang, Y. Chen, G. Zhu, J. Wang, and H. Lu, "Improving multiple object tracking with single object tracking," in *Proceedings of the IEEE/CVF Conference on Computer Vision and Pattern Recognition*, 2021, pp. 2453–2462.
- [74] P. Bergmann, T. Meinhardt, and L. Leal-Taixé, "Tracking without bells and whistles," in *Proceedings of the IEEE/CVF International Conference on Computer Vision*, 2019, pp. 941–951.
- [75] D. Stadler and J. Beyerer, "On the performance of crowd-specific detectors in multi-pedestrian tracking," in *2021 17th IEEE International Conference on Advanced Video and Signal Based Surveillance (AVSS)*. IEEE, 2021, pp. 1–12.